

LOW-TEMPERATURE HEAT CAPACITY OF MAGNESIOFERRITE, MgFe_2O_4

A. I. Turkin¹, V. A. Drebushchak^{1,2,3*}, Yulia A. Kovalevskaya² and I. E. Paukov²

¹Institute of Geology and Mineralogy SB RAS, Pr. Ak. Koptyuga, 3, Novosibirsk 630090, Russia

²Institute of Inorganic Chemistry SB RAS, Pr. Ak. Lavrentieva, 3, Novosibirsk 630090, Russia

³Novosibirsk State University, Ul. Pirogova 2, Novosibirsk 630090, Russia

Heat capacity of stoichiometric homogeneous spinel MgFe_2O_4 was measured from 5 to 305 K and thermodynamic functions were derived for temperatures up to 725 K using our previous high-temperature experimental data for the same sample.

Anomaly in C_p was found at very low temperatures. Experimental data below 20 K contain large (up to 25% near 5 K) error arising from the difference in the thermal history between the experimental series.

Magnetic contribution to the low-temperature heat capacity was tested, and the linear function was found to fit experimental data better than the three-halves power derived from the spin-wave theory.

Keywords: heat capacity, magnetic contribution, MgFe_2O_4 , phase transition, spinel

Introduction

Magnesioferrite, MgFe_2O_4 , is a magnetic mineral with the structure of inverted spinel. Its properties are very important for petrology and mineralogy of the associations deep in the Earth. Nevertheless, thermodynamic data for magnesioferrite are absent in literature. Its heat capacity was measured in a temperature range of 53 to 296 K [1], and the enthalpy increments were measured in a temperature range from 363 to 1827 K by using drop calorimetry [2]. The works were carried out especially for the thermodynamics of minerals, but the results are not used in contemporary thermodynamic database [3, 4].

The lack of reliable thermodynamic data for magnesioferrite is the result of the difficulties with the sample preparation. It is a refractory material. Direct synthesis $\text{MgO} + \text{Fe}_2\text{O}_3 \rightarrow \text{MgFe}_2\text{O}_4$ can be carried out only at very high temperatures. On the other hand, Fe changes its valency according to the scheme $\text{Fe}_2\text{O}_3 \rightarrow \text{Fe}_3\text{O}_4 \rightarrow \text{FeO}$ with temperature increasing, and the product of the synthesis under ambient pressure is nonstoichiometric, forming solid solutions $\text{MgFe}_2\text{O}_4 - \text{Fe}_3\text{O}_4$ with the excess of Fe as compared with pure MgFe_2O_4 . Magnesioferrite can be synthesized also after the decomposition of more complex minerals, but the product is not appropriate for the calorimetric measurements because it is not pure phase [5].

Heat capacity of nonstoichiometric magnesioferrite $\text{Mg}_{0.82}\text{Fe}_{2.18}\text{O}_4$ was measured at extremely low temperatures (1.8–5 K) in order to clarify the equation

for the magnetic contribution to the heat capacity of several spinels [6].

Homogeneous stoichiometric magnesioferrite was synthesized in bulk for the first time after special procedure usually used for sulfides [7] and readily adopted for oxides of 3d elements [8]. Its heat capacity was measured at elevated temperatures near the magnetic phase transition [8]. These data are not enough for the evaluation of thermodynamic functions of magnesioferrite because the entropy at 298.15 K can be derived only after low-temperature heat capacity measurements.

The objective of this work was to measure low-temperature heat capacity of magnesioferrite and to derive its thermodynamic functions.

Experimental

Spinel MgFe_2O_4 for the heat capacity measurements was synthesized at 1373 K from oxides MgO and Fe_2O_3 using silica-tube technique with intermediate grinding. The product was a fine powder, with the grains of about $5 \cdot 10^{-3}$ mm in size. According to X-ray powder diffraction, the unit cell parameter is 0.8397 nm and the inversion parameter is 0.75. The synthesis was described in details in [8].

Heat capacity was measured using the calorimetric system described elsewhere [9, 10]. The calorimeter of the internal volume of 5.7 cm^3 with magnesioferrite (3.3627 g) was evacuated and then filled with helium up to the pressure of 30 mm of Hg.

* Author for correspondence: dva@uiggm.nsc.ru

High-temperature thermodynamic functions of magnesioferrite were derived from the heat-capacity measurements on DSC-204 (Netzsch), published in [8]. Accuracy of C_p was estimated $\pm 2\%$ near 400 K and $\pm 3\%$ near 700 K.

Results and discussion

Heat capacity below 300 K

Heat capacity was measured in 94 points of a temperature range from 5 to 302 K. Experimental data are

listed in Table 1. The standard deviation is about 13% for the temperature range of 5–15 K, 4% for 15–25 K, 0.5% for 25–75 K and 0.06% above 75 K. The inaccuracy is too large at very low temperatures, much greater than those for other substances measured at the same calorimeter. It is very unusual, because the total heat capacity of magnesioferrite is greater than that of the other substances.

The reason for the large heat capacity and large inaccuracy in magnesioferrite is the same: low-temperature magnetic anomaly. Heat capacity of $MgFe_2O_4$ is shown in Fig. 1 as C_p/T vs. T^2 . It does not

Table 1 Experimental heat capacities of $MgFe_2O_4$ (formula mass=199.997 g)

T/K	$C_p(T)/J \text{ mol}^{-1} \text{ K}^{-1}$	T/K	$C_p(T)/J \text{ mol}^{-1} \text{ K}^{-1}$	T/K	$C_p(T)/J \text{ mol}^{-1} \text{ K}^{-1}$
	Series 1	7.87	0.179	59.68	15.18
295.70	146.64	9.23	0.247	64.68	18.17
298.71	147.56	10.38	0.297	69.70	21.37
301.68	148.46	11.12	0.334	74.70	24.58
	Series 2	12.31	0.389	79.67	28.01
83.13	30.33	13.60	0.464	84.66	31.47
88.17	33.93	14.75	0.536		Series 5
93.24	37.66	15.94	0.655	4.96	0.045
98.29	41.44	17.22	0.769	4.98	0.070
104.33	45.88	18.54	0.875	5.57	0.110
111.34	51.11	19.87	1.040	5.96	0.114
118.31	56.24		Series 4	6.59	0.158
125.29	61.45	5.68	0.072	7.33	0.191
132.32	66.49	6.79	0.128	8.19	0.258
139.27	71.37	8.44	0.213		Series 6
147.60	77.09	10.42	0.336	5.08	0.067
157.46	83.65	11.36	0.380	5.71	0.108
167.34	89.90	12.55	0.433	6.52	0.138
177.24	95.90	13.86	0.496	7.09	0.187
187.21	101.62	15.23	0.609	7.75	0.211
197.09	106.94	18.29	0.899	8.37	0.263
206.92	112.07	19.89	1.064	8.86	0.287
216.78	116.61	21.54	1.267	11.98	0.462
226.62	121.23	23.20	1.524	13.58	0.596
236.52	125.41	25.47	2.003	16.67	0.827
246.41	129.40	28.10	2.486	18.30	0.923
256.31	133.19	30.70	3.087	22.38	1.512
266.30	136.82	33.30	3.776	24.46	1.804
276.23	140.25	35.88	4.529	26.59	2.203
286.11	143.44	38.49	5.334	28.74	2.617
296.03	146.60	41.87	6.653		Series 7
	Series 3	45.93	8.317	46.50	8.70
5.50	0.065	50.01	10.13	50.54	10.50
6.82	0.128	54.61	12.45		

obey the Debye model at very low temperatures. Experimental values fit to a straight line that does not cross the zero point. The functional relation changes below 9 K (80 K^2 on the x -axis), and the heat capacity decreases rapidly with temperature. Heat capacity data for isostructural spinel MgAl_2O_4 without magnetic interaction are shown in the same figure with a solid line, indicating evidently the magnetic contribution in the C_p of MgFe_2O_4 . It is well seen in Fig. 1 that the large standard deviation is caused by the difference between various series (systematic bias), not by random errors. Such an increase in the standard deviation was discussed as the main reason of the enlarged uncertainty in the heat capacity of magnetic materials, when various samples are measured [11]. For a single sample, extremely large amplitude of this effect was detected in the magnetic solid solution $\text{Fe}_{0.96}\text{S}-\text{Ni}_{0.96}\text{S}$ near the point of the discontinuity in the magnetic ordering [12]. Here we see the difference in the heat capacity of the same sample near to the magnetic anomaly range. The greatest difference in the heat capacity between the series is about $\pm 25\%$ near 5 K. Fortunately, this kind of uncertainty in the heat capacity decreases with increasing temperature and vanishes above 20 K. Considering the uncertainty in the enthalpy and entropy of $\pm 25\%$ at 20 K (conservative error estimate), we receive the contribution in the uncertainty at 298.15 K of about 0.1% for entropy and 0.01% for enthalpy. The smoothed values of heat capacity and derived enthalpy and entropy are in Table 2. Below 5.5 K, the heat capacity was extrapolated to zero temperature by using cubic function $C_p(T)=C_p(5.5) (T/5.5)^3$.

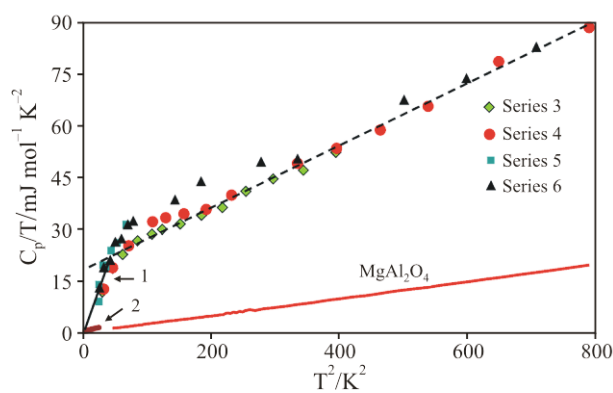


Fig. 1 Low-temperature heat capacity of MgFe_2O_4 spinel, plotted as C_p/T vs. T^2 (different marks for different series). — Magnetic contribution to its heat capacity is evident in comparison with $C_p(T)$ for non-magnetic MgAl_2O_4 spinel. - - - an eye guide to show the linear behavior. Arrows indicate 1 – line of the extrapolation to zero temperature and 2 – heat capacity of nonstoichiometric spinel $\text{Mg}_{0.82}\text{Fe}_{2.18}\text{O}_4$

Heat capacity above 300 K

Heat capacity of magnesioferrite (the same sample) in a temperature range from 430 to 720 K was published in [8], but without thermodynamic functions. Now we have low-temperature heat capacity and can calculate entropy and enthalpy from 300 to 720 K. Low-temperature data are more accurate (accuracy of about 0.2%, derived from the measurements of the reference

Table 2 Low-temperature thermodynamic functions of MgFe_2O_4 (formula mass 199.997 g mol⁻¹)

T/K	$C_p(T)/\text{J mol}^{-1} \text{K}^{-1}$	$H(T)-H(0)/\text{J mol}^{-1}$	$S(T)/\text{J mol}^{-1} \text{K}^{-1}$
5	0.061	0.077	0.020
10	0.30	1.01	0.14
15	0.56	3.21	0.31
20	1.05	7.31	0.55
25	1.91	14.61	0.87
30	2.91	26.55	1.30
35	4.25	44.32	1.85
40	5.91	69.6	2.52
45	7.91	104.1	3.33
50	10.21	149.3	4.28
60	15.35	276.3	6.58
70	21.47	459.9	9.40
80	28.21	708	12.70
90	35.29	1025	16.43
100	42.67	1415	20.53
110	50.12	1879	24.94
120	57.52	2417	29.62
130	64.81	3028	34.51
140	71.89	3712	39.58
150	78.72	4465	44.77
160	85.26	5285	50.06
170	91.53	6170	55.42
180	97.49	7115	60.82
190	103.15	8118	66.25
200	108.47	9177	71.67
210	113.50	10287	77.09
220	118.21	11446	82.48
230	122.66	12650	87.83
240	126.85	13898	93.14
250	130.80	15186	98.40
260	134.58	16514	103.61
270	138.11	17877	108.75
280	141.52	19275	113.84
290	144.76	20707	118.86
298.15	147.30	21897	122.91
300	147.87	22170	123.82

substances, i.e., benzoic acid, corundum, copper) than high-temperature ones (~2%). Fitting upper five points of smoothed C_p values in Table 2 with five lower points of C_p published in [8], we used polynomial $C_p = a_0 + a_1 T^{-1} + a_2 T^{-2} + a_3 T^{-3}$, varying simultaneously the calibration coefficient for the high-temperature values. Similar procedure was used in [13], but with overlapping low- and high-temperature data. Here, there is a temperature gap of about 130 K between low- and high-temperature values. Coefficients a_i and the calibration factor in the fitting are calculated analytically, using the least squares procedure. The best fitting corresponds to the decrease in the C_p values measured with DSC by 1.6%. As this value is within the limits of the reported experimental error ($\pm 2\%$), we consider the decrease by 1.6% as the correction. The polynomial fits five low-temperature points with the standard deviation less than 0.01% and five high-temperature points less than 0.03%. This is within the limits of rounding.

Low- and high-temperature heat capacities fitted together are shown in Fig. 2. Smoothed values of $C_p(T)$ and derived entropy and enthalpy are listed in Table 3.

Comparison with literature data

High-temperature heat capacity of magnesioferrite was derived by Bonnickson [2] from his own enthalpy measurements. Enthalpy increments were fitted to the second-order polynomial below 665 K and the first-order polynomial from 665 to 1230 K. Temperature of 665 K was considered to be the phase transition point. Heat capacity in [2] is a linear function of T below 665 K and a constant above. Our experimental data for $C_p(T)$ show the lambda-anomaly, having nothing to do with the triangle shape used by Bonnickson [2]. It is meaningless to compare these different heat capacity functions. One can compare

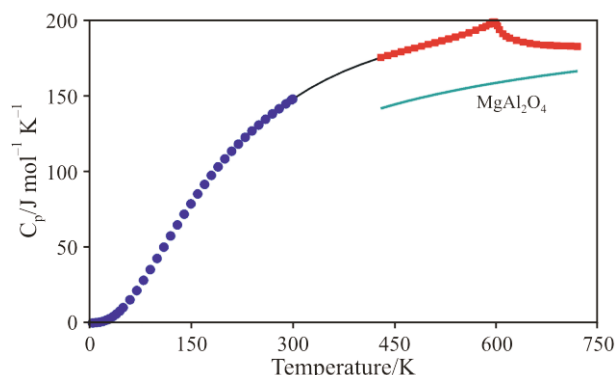


Fig. 2 Fitting low- and high-temperature heat capacities of magnesioferrite (line). Marks show the smoothed C_p values. Heat capacity of non-magnetic spinel $MgAl_2O_4$ is shown (solid line)

Table 3 High-temperature thermodynamic functions of $MgFe_2O_4$ (formula mass 199.997 g mol $^{-1}$)

T/K	$C_p(T)/$ J mol $^{-1}$ K $^{-1}$	$H(T)-H(0)/$ J mol $^{-1}$	$S(T)/$ J mol $^{-1}$ K $^{-1}$
298.15	147.30	21897	122.91
300	147.87	22170	123.82
325	154.9	25956	135.9
350	160.9	29906	147.6
375	166.2	33997	158.9
400	170.7	38209	169.8
425	174.6	42526	180.3
450	177.9	46934	190.4
475	181.0	51420	200.1
500	184.0	55983	209.4
525	187.0	60620	218.5
550	190.3	65335	227.3
575	194.2	70140	235.8
597	198.8	74462	243.2
600	197.7	75057	244.2
625	187.4	79831	252.0
650	184.6	84477	259.3
675	183.4	89075	266.2
700	183.0	93656	272.9
725	182.6	98226	279.3

the transition points instead. It is 597 K in our report [8] and 665 K in [2]. The difference is too large. The reason, we think, is nonstoichiometric sample of Bonnickson [2] and King [1]. It was mentioned in the Introduction that the nonstoichiometric samples are solid solutions of the $MgFe_2O_4$ – Fe_3O_4 series. Magnetic phase transition for pure Fe_3O_4 is at much higher temperature, ranging from 848 K [4] to 858 K [14]. Thus, one can conclude that the impurity of Fe_3O_4 in the sample of Bonnickson [2] moved the transition point toward high temperatures by 65 K.

Peak at 597 K is the transition from ferrimagnetic to paramagnetic state. It was discussed in [8]. Low-temperature anomaly near 10 K was never detected before, because heat capacity was never measured at extremely low temperatures so far, as well as magnetic properties.

Heat capacity measured at low temperatures by King [1] is 2.5% less than ours near 298 K. The difference increases with decreasing temperature [1] and at 63 K (the lowest temperature in [1]), is about 7%. Derived entropy at 298.15 is 3.7% less than our value in Table 2.

Heat capacity data for nonstoichiometric magnesioferrite measured at extremely low temperature in [6] are about eight times less than ours at 5 K.

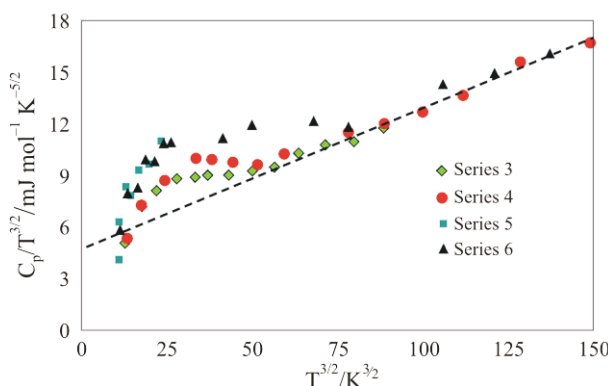


Fig. 3 Testing the three-halves power magnetic contribution to the heat capacity derived from the spin-wave theory. Low-temperature heat capacity of MgFe_2O_4 spinel is plotted as $C_p/T^{3/2}$ vs. $T^{3/2}$ (different marks for different series). Dashed line is an eye guide to show the linear behavior

This temperature is the high limit of the measurements in [6], and the low limit in our measurements. The whole difference in the heat capacity is evidently due to the magnetic contribution. It is evident from Fig. 1, where C_p of $\text{Mg}_{0.82}\text{Fe}_{2.18}\text{O}_4$ is close to that of nonmagnetic MgAl_2O_4 .

Function $C_{p,m}=aT^{1.5}$ for the magnetic contribution was derived from the spin-wave theory, predicted by Bloch [15]. It is very interesting to compare the three-halves power function with the conventional function $C_{p,m}=aT$ used in calorimetry. Linear function is very suitable for practice, for it allows one to detect ferroelectric, ferromagnetic or electronic contributions at once, in the uniform procedure, using a C/T vs. T^2 plot. It is shown in Fig. 1 for our data. After comparison of Figs 1 and 3, we prefer the linear function. It seems to fit the experimental data on heat capacity with magnetic interaction better. One can anticipate that the same conclusion would be made if the linear function instead of the three-halves one is used in the analysis of low-temperature heat capacity of other compounds with spinel structure [16].

Conclusions

Synthesis of pure homogeneous magnesioferrite MgFe_2O_4 allowed us to measure its low-temperature heat capacity and, together with the previous high-temperature measurements, to derive reliable thermodynamic functions. They differ from the data published about 50 years ago, because that sample was probably the solid solution of the MgFe_2O_4 – Fe_3O_4 series. Largest difference is in the magnetic transition point: 597 K (our) instead of 665 K (literature).

At very low temperature, heat capacity of magnesioferrite has a magnetic contribution, increasing

linearly with temperature. The attempt to use the three-halves power derived from the spin-wave theory was unsuccessful. Experimental points fit the straight line $C_p/T^{3/2}$ vs. $T^{3/2}$ worse than C_p/T vs. T^2 .

Irreproducibility in the magnetic properties of the sample after heating–cooling cycles during the experiments produces large irreproducibility in the heat capacity between different series of the measurements.

Acknowledgements

The work was supported by RFBR grants 05-05-64556 and 06-05-65114. It was partly supported by the Integration Interdisciplinary Project N 81 of the Siberian Branch of the Russian Academy of Sciences.

References

- 1 E. G. King, J. Am. Chem. Soc., 76 (1954) 5849.
- 2 K. R. Bonnickson, J. Am. Chem. Soc., 76 (1954) 1480.
- 3 R. A. Robie and B. S. Hemingway, U.S. Geological Survey Bull., 2131 (1995) 461.
- 4 S. K. Saxena, N. Chatterjee, Y. Fei and G. Shen, An Assessed Data Set Based on Thermochemistry and High Pressure Phase Equilibrium, Springer-Verlag, Berlin 1993, p. 428.
- 5 R. L. Frost, J. M. Bouzaid, A. W. Musumeci, J. T. Kloprogge and W. N. Martens, J. Therm. Anal. Cal., 86 (2006) 437.
- 6 S. R. Pollack and K. R. Atkins, Phys. Rev., 125 (1962) 1248.
- 7 V. A. Drebushchak, T. A. Kravchenko and V. S. Pavlyuchenko, J. Cryst. Growth, 193 (1998) 728.
- 8 A. I. Turkin and V. A. Drebushchak, J. Cryst. Growth, 265 (2004) 165.
- 9 I. E. Paukov, I. A. Belitzky and Yu. A. Kovalevskaya, J. Chem. Thermodyn., 33 (2001) 1687.
- 10 V. G. Bessergenev, Yu. A. Kovalevskaya, L. G. Lavrenova and I. E. Paukov, J. Therm. Anal. Cal., 75 (2004) 331.
- 11 V. A. Drebushchak and A. I. Turkin, J. Therm. Anal. Cal., 90 (2007) 795.
- 12 V. A. Drebushchak and E. F. Sinyakova, J. Therm. Anal. Cal., 89 (2007) 303.
- 13 V. A. Drebushchak, Yu. A. Kovalevskaya, I. E. Paukov and E. V. Boldyreva, J. Therm. Anal. Cal., 85 (2006) 485.
- 14 R. E. Newham, In: The Encyclopedia of Mineralogy, K. Frye, Ed., Hutchinson Ross Publishing Company, Stroudsburg, Pennsylvania 1981, pp. 226., 794.
- 15 F. Bloch, Z. Phys., 61 (1930) 206.
- 16 N. W. Grimes, Proc. R. Soc. London, A338 (1974) 209.